High Densities and Low Filling Factor

Giovanni Peres

Istituto ed Osservatorio Astronomico di Palermo, Piazza del Parlamento 1, 90134 Palermo, ITALY

Abstract. This paper discusses the evidence of very high coronal plasma density, i.e. up to 10^{12} cm^{-3} and higher, sometimes measured with spectroscopic diagnostic methods during flares and in active regions. The ratio of the forbidden and intercombination lines in He-like ions has been the most used spectroscopic tool in such measurements. The limits and advantages of spectroscopic diagnostics are discussed as well as the interpretation of such high density, both in terms of high density filamentation and, with the help of hydrodynamic model calculations, in terms of of chromospheric evaporation and dense plasma layers in the transition region of flares.

1. Introduction

This paper reviews the evidence of very high coronal density, derived from X-ray spectroscopic measurements at high resolution which has been sometimes related to the fine structuring of the solar outer atmosphere, the main subject of this workshop. Indeed measuring, with a spectroscopic diagnostic method, a density much higher than what typically derived in the corona, with other methods, e.g. from X-ray images collected with Skylab/S054 and Yohkoh/SXT, may imply that the line emitting plasma is clumped in small structures, unresolved in the X-ray images, with a very small filling factor and raise the question on whether there is a magnetic structuring of the plasma much finer than so far observed or not. More specifically, since the emissivity of the collisionally excited coronal plasma is proportional to the square of the density times the volume, a density higher by a given factor, for the same emitted flux, implies a volume smaller by the square of the same factor and therefore a smaller filling factor.

The band ratio method applied to X-ray images taken in different bands yields the average plasma temperature inside a pixel from the ratio of the flux in the two bands; the emission measure is then derived from the known plasma radiative efficiency filtered by the instrument; finally, assuming the geometry of the optically thin plasma in the pixel, the density is obtained. The assumption on geometry involves both the depth of the emitting plasma along the line of sight and the filling factor of the plasma inside the pixel. For instance one may assume that the plasma extends along the line of sight as much as the thickness of the observed loop(s) or as much as the sixe of the observing pixel. [1] It is invariably assumed that the plasma is uniform within the observed pixel. The typical density derived with this method is between 10^9 cm^{-3} and 10^{10} cm^{-3} in the active regions; and between 10^{10} cm^{-3} and 10^{11} cm^{-3} in flares. A value of 10^{11} cm^{-3} in big flares is not unusual.

On the other hand the analysis of density sensitive lines collected by spectroscopic instruments, such as XRP/SMM and SOLEX/P78, with $E/\Delta E$ slightly less than 10^4 and limited, or no, angular resolution has sometimes given evidence of density in excess of 10^{11} and, in some cases, up to 10^{13}, during some flares. The density significantly higher (100 times) than what typically measured with other methods is, therefore, claimed as evidence for a 10^4 times smaller emitting volume.

In this respect it is worth noting that any improvement in the resolution of coronal X-ray images has invariably shown, so far, finer and finer structuring. The very first observations, with very coarse angular resolution, showed an apparently almost uniform corona with an average density close to 10^8 cm^{-3}. As the resolution of the images improved, finer and finer details emerged: initially entire active regions were visible, then the finer structures inside active regions and in the quiet Sun; eventually individual loops were detected with rocket-borne telescopes (Vaiana, Krieger and Timothy, 1973), then with Skylab/S054 (Vaiana et al. 1973) and Yohkoh/SXT (cf. the book edited by Uchida, Watanabe, Shibata and Hudson, 1994). NIXT images (Golub et al., 1990) prove unequivocally the existence of even finer structuring in the corona, down to the arcsec and, in particular, the work of Gomez, Martens and Golub (1993) has analysed the characteristic sizes of the structures present in images of active regions taken by NIXT. Gomez et al. show the existence, in all the active regions, of structures of all sizes down to the arcsec size, i.e. the resolution limit of film used for NIXT images; the spatial Fourier transform yields for any active region invariably a power law spectrum down to the resolution limit, clearly suggesting that it may continue well below the arcsec range. In other words structuring well below the arcsec can easily be present in the solar corona.

Spectroscopic measurements of high density may give independent evidence of small scale structuring; however, it is also worth noting that such measurements have a non-obvious interpretation. The density determination, or its interpretation, has been accepted by some but also taken with scepticism by others, as this review will discuss, attempting to incorporate and to discuss various opinions.

2. The spectroscopic diagnostics of Density

2.1. The He-like ions

A significant part of the diagnostics of density through spectroscopy here discussed is based on the work by Gabriel and Jordan (1969, 1972) who showed

[1] The latter assumption has been made also when deriving the filling factor in some of the papers here discussed.

how the ratio between the intensity of intercombination and forbidden lines in He-like ions is density sensitive.

The diagnostics works, schematically, as follows: for low plasma density the $1s2s\ ^3S_1$ level is fairly populated with respect to the other levels; the transitions from this level to the ground level $1s^2\ ^1S_0$ yield the forbidden f line of fundamental importance here. For higher and higher density, collisions depopulate more and more this level and populate the $1s2p\ ^3P_{1,2}$ level, the transitions from this level to the ground level yield the intercombination i line; for higher density, therefore, the forbidden line gets weaker while the intercombination line stronger; the ratio $R = f/i$ of the two lines yields, therefore, a diagnostics of the electron density, above a threshold density which depends on the specific ion. The resonance r line is due to transitions from the $1s2p\ ^1P_1$ level to the ground level and the ratio $G = (f+i)/r$ yields a diagnostics of the temperature.

Table 1 lists the He-like ions of importance in coronal conditions, along with the temperature of maximum ion formation in equilibrium conditions and the critical density N_c defined according to the formula $N = N_c(R_0/R - 1)$ where N is the ambient electron density, R_0 is the low density value of the line ratio and $R = f/i$.

From Table 1 it is easy to see that the ions forming at higher temperatures cannot, in practice, provide a density diagnostics because their threshold density is too high. A diagnostic of density can be obtained only up to the Mg XI ion and, therefore, for temperatures $\approx 6 \times 10^6$ K or slightly higher. Fig. 1 illustrates the diagnostic potential of such a method for the three coolest coronal ions.

Table 1. Coronal He-like ions.

Ion	T_{max} (10^6 K)	N_c(cm^{-3})
O VII	2	3×10^{10}
Ne IX	4	6×10^{11}
Mg XI	6	3×10^{12}
Si XIII	10	1.3×10^{13}
S XV	20	8.9×10^{13}
Ca XIX	30	2×10^{16}
Fe XXV	70	7×10^{17}

While the general features of the diagnostics are well established, the solar observations have helped to refine the atomic physics parameters, e.g. R_0, through direct measurements, since both theoretical calculations and laboratory experiments are fairly complicated for such ions (cf., for instance, Wolfson, et al. 1983, or Linford, Lemen and Strong, 1991)

2.2. Other spectroscopic density diagnostics

Other diagnostic using X-ray density sensitive lines have been adopted; since they have been applied only to specific observations, they are discussed briefly where appropriate.

3. High Density Measurements in Flares

There was a set of works, following the paper by Gabriel and Jordan (1969), reporting high density in active regions or flares (e.g. Walker and Rugge, 1970; Freeman et al., 1971). Such works, however, were based on R measurements compromised by several factors, such as low spectral resolution and the presence of other lines.

It is worth noting that, for instance, for the O VII complex at least a resolution of $E/\Delta E = 120$ is required. The spectra here discussed have a much higher resolution, being taken with Bragg Crystal Spectrometers scanning the spectra with $E/\Delta E$ up to about 10^4.

McKenzie et al. (1980) successfully used the O VII complex measurements, made with the Solex B spectrometer on board the satellite P78-1, during the June 10, 1979 flare: the density measured with R and pertaining to the temperature of a few 10^6 K typical of O VII, grew even after the flare brightest phase and reached a maximum value of 1.7×10^{11} cm^{-3}, a high but not extremely high value.

Also Doschek et al. (1981) applied the He-like O VII ion line diagnostics to the observations of the April 8, 1980 flare, an M class flare, made with the same instrument; Fig. 2 shows some results of their analysis. The density, as derived from the O VII lines, rises steeply during the rise phase of the O VII light curve, then it decreases, first rapidly and afterwards more gradually. The maximum density value in the April 8, 1980 flare is 2×10^{12} cm^{-3}. While only one spectral measurements yields a density above 10^{12} cm^{-3}, five data points are at a few 10^{11} cm^{-3} and only after 10 minutes (≈ 10 measurements) the density appears to go below 10^{11} cm^{-3} (therefore high density values do not appear to occurr by chance in a measurement and the same is true for the following works).

The same paper shows similar results for the May 9, 1980 flare, also of M class. The density in such a flare rises to almost 10^{12} cm^{-3}, and after a rapid decrease it remains at a few 10^{11} for almost 10 minutes. Both the rise and decay phase of both flares appear to be well covered. The line flux measurement allows to derive, simultaneously, the emission measure. Since both the density and the emission measure are simultaneously known then the emitting volume and the total number of ions involved can be obtained. The volume of the O VII emitting plasma increases during the decay of the density by more than a factor 10^7. The authors interpret such an expansion as the chromospheric evaporation, i.e. the rapid expansion into corona of the plasma on top of the chromosphere over-heated to a few million degrees. Simultaneous measurements of other lines (Ca XIX, Fe XXV and OVIII complexes) allowed to study the multithermal structure of the plasma.

Such flares have driven much interest from the solar community because of their particularly good time coverage and the availability of simultaneous observations in several bands. They were reanalized, along with the February 26, 1981 14:24 UT flare by Bruner et al. (1988), taking into account a more refined and updated instrumental response, as well as additional observations in the microwave and the hard X-ray bands. Also for the February 26, 1981 flare the O VII line diagnostics yield peak density values of up to 10^{12} cm^{-3}. The work by Bruner et al., in particular, focused on the evolution of the density and the volume of the O VII emitting plasma; in this respect attention was paid to the effect of subtracting the pre-flare emission, less conspicuous than the flare one, but normally present for such a cold line. The point the authors want to make is that such a subtraction allows to remove the significantly larger volume of the preflare emitting region and, thus, to derive an average density value larger than obtained not removing the preflare emission. However the finding were in agreement with those of Doschek et al.. They also interpret the volume evolution of the O VII emitting plasma in terms of the filling of a flaring loop by the plasma evaporating from the chromosphere.

Even higher density values were inferred by Linford and Wolfson (1988) for the C3 flare of May 21, 1985, observed with the FCS/XRP spectroscope on board the XMM satellite during the flare observation. The instrument was first used to make space and time resolved observation in several X-ray lines during the pre-flare and impulsive flare phases; it was then used to scan repeteadly the Mg XI and Ne IX resonance, forbidden and intercombination line complexes, maintaining its pointing fixed on the point of the flare brighter in the previous images taken in the Mg XI line. The part of their results dedicated to density measurements, shown in Fig. 3, show a monotonic decay of density from initially high value. The first density value reported for Mg XI is 5×10^{12} cm^{-3}, shortly before the maximum of the Ca XIX spatially integrated light curve, and it decays to 10^{12} cm^{-3} in slightly less than 10 minutes. The density values inferred from the observations of the cooler Ne IX line, during the same flare, appear slightly but not significantly lower and, apart from a single data point, are not incompatible with observing essentially the same plasma. Also the temperature profile derived from the two ions lines, shows a consistent behaviour between the two spectral complexes and the same evolution.

Zarro, Slater and Freeland (1988) report, for the May 24, 1987 flare, observed with the same instrument, a 5×10^{12} cm^{-3} density derived from the Mg XI spectrum, along with a blue shift interpreted as the signature of chromospheric evaporation at low coronal temperature.

Linford, Lemen and Strong (1991) made a statistical analysis of 50 spectral scans of the Mg XI line complex made during 18 flares; in 14 spectra, taken during the flare decay phase, they found a density significantly higher than the low density limit, i.e. at 10^{12} cm^{-3} or higher, up to 10^{13} cm^{-3} in one case. The spectroscopic measurements were also devoted to a more accurate determination of R_0, the low density limiting value of R, for Mg XI. The simultaneous knowledge of the emission measure allowed them to derive the emitting volumes which turned out to be very small, if compared to typical flare volumes or to the cube of the pixel's linear size. [2] They ranged between 5.4×10^{23} cm^3 and 10^{21} cm^3. Such values correspond, respectively, to the lowest and the highest density values.

While the spectroscopic measurements mentioned above refer to intermediate plasma temperature (below 10^7 K) during a flare, more recently, Phillips et al. (1996) have tried to determine the density also of the hotter plasma in flares, taking advantage of spectral scans made with FCS/XRP on board XMM

[2] One can estimate an observed volume by considering the area on the Sun filling the observing resolving element and a height above it approximately equal to the linear size of the resolution element.

of the density sensitive line complexes of Fe XXI (between 9.4 A and 9.8 A) and Fe XXII (between 8.95 A and 9.1 A) forming around 10^7 K, during the M4.5 flare on 1985, July 2, 21:11. The Fe XXII spectral complex was scanned around 21:28, just after the flare maximum, and the Fe XXI was scanned a few minutes later, 21:32-21:35 UT. Exploiting such a diagnostic involved the quite substantial task to calculate anew the atomic physics parameters for the relevant levels and transitions, to synthesize a set of spectra for various plasma parameters and then to derive the conditions of the observed plasma determining which of the synthesized spectra better compared with the observed ones.

The comparison of observed and synthesized spectra, reported in Fig. 4, shows that the Fe XXII scan is more consistent with a density around 10^{13} cm^{-3}, while the Fe XXI scan, made later during the flare decay is consistent with a density around 10^{12} cm^{-3}. The volume effectively emitting the Fe lines turns out to be much smaller than the volume derived from the cube of the pixel linear size, raising again the issue of small filling factor. The authors claim that such measurements are in agreement with the idea of very thin filamentation of the dense emitting plasma.

4. Hydrodynamic Models and High Density

An explanation, alternative to that of filamentation, has been that such high density values originate in the process of chromospheric evaporation and that the high density plasma is just that of the over-heated chromospheric upper layers. In the following I will discuss such a hypothesis in more detail by means of hydrodynamic models of flaring loops. We have used the new version of the Palermo-Harvard hydrodynamic loop model (Peres et al. 1982; Betta et al. 1997) capable of maintaining high spatial resolution in the transition region, at all times, through a dynamic regridding algorithm; the new code can also solve non-symmetrical loop hydrodynamic problems but for the present purposes a symmetric loop model suffices. In the calculations here discussed we consider a flaring loop, semicircular and of constant cross section, with a semilength of 2×10^9 cm, initial coronal pressure ≈ 6 dyn cm^{-2} and maximum coronal temperature before the flare 3.2×10^6 K.

We have first modelled an impulsive heat release in the coronal part of the loop, with a sudden turn on and lasting continuosly for 180 s, the spatial distribution is gaussian, centered at the loop apex, with a $\sigma = 5 \times 10^8 cm$, and maximum intensity 10 erg cm^{-2} s^{-1}. As time progresses the maximum temperature, and the temperature in any part of the corona, increases. The temperature distribution in this solution is always monotonically increasing along the loop, from the footpoints to the loop apex. Also the density increases at all the points as a consequence of the chromospheric evaporation. As the "flare" progresses, the density increases at the temperature of maximum ions formation, reaching beyond the 10^{11} cm^{-3} level for all three ions. The temperature of formation of such ions, during a flare, actually is in the very steep transition region and, therefore, a rather geometrically thin plasma layer is involved in emitting the line. The small volumes found in the He-like line measurements could, therefore, be just very flat plasma layers which emit the lines.

Releasing an heating ten times larger (maximum intensity 100 erg cm^{-2} s^{-1}) and leaving all the other characteristics unchanged, the temperature rises even more, by a factor of two, and the chromospheric evaporation is more vigorous. In Fig. 5a we show the evolution of plasma density vs. plasma temperature, every second, over 146 s from the beginning of the heat release; the flare heating is continuously on during the evolution here shown. The steadily increasing density at the temperature of the three lines formation goes beyond 10^{12} cm^{-3} and almost reaches 10^{13} cm^{-3} for the O VII line.

We also calculated the evolution of flaring loops heated near the loop base with heating sufficient to reach peak temperature very close to those of heating at the loop apex. The plasma density at the temperature of the line formations is even higher than in the previous cases, since the evaporation is more strongly driven by the base heating. Also in this class of calculations, the more intense the heating, the higher is the density at the temperature of the line formation. Fig. 5b shows the evolution of density vs. temperature in a flaring loop with the same initial conditions as above, with a heating centered at the base of the corona with a gaussian spatial distribution of maximum intensity 10^3 erg s^{-1} cm^{-3} and $\sigma = 3.33 \times 10^7$ cm. The heating is continuosly on during all the evolution of 102 s shown; the results are plotted with a frequency of one second. After approximately 20 s since the beginning of the heating, also in this case the temperature monotonically increases along the loop at any time.

Flares can certainly be a more complex phenomenon than this model describes, with many loops in different condition heated and emitting simultaneously; also the lines form over a range of temperatures and the plasma at each temperature contributes according to the emission measure at that temperature. Therefore the density measured in each line is a weighted average of the various magnetic loops involved. However it clearly appears that the high density values found could be explained with the plasma stratification and evolution of flaring loops subject to chromospheric evaporation, as described by hydrodynamic loop models. On one hand hotter loops tend to have higher density because of more intense evaporation and, also, the He-like lines which allow the density measurements are typically formed in the transition region of the flaring loops, where the density is even higher than in the coronal part of the flare.

Therefore rather than attributing the high density to the entirety of the flare we should consider that the volume emitting the lines so far measured is indeed small and at high density but it is just in the transition region of the entire coronal flaring volume, the hottest part being at lower density.

5. Density Measurements in Active Regions

The density values in active regions derived from the X-ray images of Skylab and Yohkoh is typically in the range of $10^9 - 10^{10}$ cm^{-3}.

Mc Kenzie (1987) made a systematic analysis of all the ARs O VII line complex scans made with SOLEX on board the satellite P78-1. Out of 111 spectra analyzed, 73 yielded a measurable R ratio. Of these only eight gave a density higher than 3×10^9 cm^{-3}. The remaining ARs yielded an average value of 2×10^9 cm^{-3}. The highest density values, i.e. a few 10^9 cm^{-3}, were measured in the ARs producing a higher rate of flares; therefore the spectroscopic density diagnostics in ARs yields values comparable to what obtained from other measurements, e.g. from X-ray images.

More recently Phillips et al. (1996), have made an original (albeit controversial) approach to the task of measuring the density in active region. Their work was based on a series of spectral scans of the Fe XVII and Fe XVI line complex between 15 and 17 A, collected, during with the FCS/XRP on board SMM, several times during 11 days for the AR 4787, as it gradually was carried by solar rotation from the central parts of the solar disk to the solar limb. From the ratio of the *measured* intensity of the Fe XVII (15.015 A), resonantly scattered in the solar plasma, with the intensity for the same line inferred from the measurements of Fe XVII (16.776 A), unscattered, and of Fe XVI (16.073) used to account for a weak temperature dependence, Phillips et al., derived the column depth $N_e l$. The simultaneous knowledge of the emission measure $N_e{}^2 l A$ plus assuming the complete filling of the beam (i.e. the instrument spatial integration element) allowed them to derive the density. Fig. 6 shows their results vs. heliocentric distance; the inaccuracy on N_e and l are claimed to be just a factor of 2. The determination of higher and higher density as the active region moved toward the limb is claimed to be caused by the deeper and deeper penetration of the line of sight into the core of active regions: at the sun center the line of sight would be intercepted by high lying loops filled with tenuous plasma, at the solar limb the line of sight would reach deep in the loops with higher density, up to almost 10^{11} cm^{-3}, located in the core of the AR. Such an interpretation is certainly arguable and the determination stands on many assumptions; however it is a quite interesting analysis and one wishes the opportunity of other independent measurements for comparison with the present one.

6. High Density Measurements in Stars

Spectroscopic measurements of stars with spectral power adequate to resolve density sensitive lines and complexes in EUV have been made by the satellite EUVE. We refer to the review by Drake (1996) on the evidence of very high density in particularly active stars. The underlying mechanism may be related to activity and therefore similar to the solar one.

7. Discussion

The determination of such high density has been subject to criticisms, e.g. the possibility that time dependent excitation may somehow alter such findings; also one wonders the extent to which the indetermination of the atomic physics parameters may still affect the results.

Furthermore these spectra have been derived scanning the line complexes and, in some cases, the time needed to perform a scan may be significantly long if the plasma conditions change rapidly, as it occurs during the early flare phases: one may therefore mix lines of the He-like complex measured at different times, so altering the significance of the R ratio. Indeed sometimes the highest density values occurr at the time of fastest change. The scans reported by Linford and Wolfson (1988), for instance, in view of this problem were taken with a faster and slightly coarser scanning mode. Such a concern may affect most significantly only the fast rise phase of the beginning and much less the more gradual decay phase. Albeit the highest density values are typically found during the early flare phases, fairly high density values are also measured during the decay phase.

One may wish to know how frequent such high densities are, i.e. whether they are an exceptional or a frequent occurrence. In this respect Linford et al. (1991) statistical work mentioned before suggests that the very high density events may not be very frequent and, furthermore, there may be a natural tendency to report the most striking events. A more accurate statistical analysis of the selection effect may be appropriate.

In spite of all the criticisms which can be raised against the high density measurements, one must note that different instruments, in several different events, from five different spectral line complexes have measured high plasma density: one therefore cannot dismiss such findings as all affected by systematic errors, in lack of a substantial counter-analysis of the data.

The interpretations of such high density measurements is more controversial: on one hand the presence of *filamentation* at high density has not been proved uniquely, albeit it may fit well in the reconnection model, and no detailed model calculation has been presented. Alternatively the high density may be explained as arising from a very thin layer in the transition region of flaring loops: in a flaring loop with 2×10^7 K maximum temperature, the plasma at 10^7 K is already in the transition region. Furthermore the chromospheric evaporation mechanism may very easily explain the connection between the high density and the high temperatures because the more intense the heating, the higher the coronal temperature but also the more intense the chromospheric evaporation and, therefore the density in corona and in the transition region.

Independently of the possible interpretations, this is the class of problems which will certainly benefit from observations at high angular and time resolution, as far as they can show the structure and evolution of the very dense plasma.

Acknowledgments. This work was partially supported by Ministero della Universitá e della Ricerca Scientifica e Tecnologica and by the Agenzia Spaziale Italiana. I acknowledge considerable help by F. Reale in producing the hydrodynamic model results.

Questions and Comments

There was a lively discussion during the workshop on the high density topic. Among the several questions and comments, only G. Emslie gave me in writing some personal comments which I will try to report briefly below. If a medium is inhomogeneous, then the line intensity (and their ratio) will reflect a highly weighted mean density in the region. Identification of a single density from such a line ratio may be problematic. (G. Emslie is to a certain extent right since the emission is proportional to the square of density so the averaging of the plasma emission in the pixel, how any instrument does, is more weighted toward the highest density parts. Highest density regions therefore may appear more prominent than they are.) Is the f/i ratio sensitive to the presence of a non-thermal population of electrons? (Some independent spectroscopists which I later questioned on this topic tend to answer "not to a large extent" and prefer the high density as an explanation) A third consideration by Emslie evaluates the thickness Δz of the transition regions in evaporation models; since such a thickness is determined by the downward conductive flux $F_c \approx T_{max}^{7/2}/\Delta z$ a ten-fold increase of temperature, as it occurs in flares, may lead to a decrease of $\approx 3 \times 10^3$ in the thickness of the line emitting region. (Such a comment is fundamentally along the same line as the hydrodynamic model results presented before.)

References

Brown, W.A., Bruner, M.E., Acton, L.W., Mason, H.E., 1986, ApJ, 301, 981

Bruner, M.E., Crannell, C.J., Goetz, F., Magun, A., McKenzie, D.L., 1988, ApJ, 334, 494

Doschek, G.A., 1990, ApJS, 73, 117

Doschek, G.A., Feldman, U., Landecker, P.B., McKenzie, D.L., 1981, ApJ, 249, 372

Drake, J.J., 1996, in Cool Stars, Stellar Systems and the Sun, Ninth Cambridge Workshop, ed. Pallavicini, R., and Dupree, A.K., PASP Conference Series, p. 203 ApJ, 249, 372

Freeman, C.P., Gabriel, A., Jones, B.B., and Jordan, C., 1971, Phil. Trans. Roy. Soc. London, 270, 127

Gabriel, A., and Jordan, C., 1969, MNRAS, 145, 241

Gabriel, A., and Jordan, C., 1972, in "Case Studies in Atomic Physics Collisions", vol. 2, ed. McDaniel E.W. and McDowell, M.R.C., Amsterdam: North Holland, p. 209

Golub, L., Herant, M., Kalata, K., Lovas, I., Nystrom, G., Pardo, F., Spiller, E., Wilczynski, J.S., 1990, Nature, 344, 842

Gomez, D.O., Martens, P.C.H., and Golub, L., 1993, ApJ, 405, 767

Linford, G.A., Lemen, J.R., Strong, K.T., 1991, Adv. Space Res., 11, (1)147

Linford, G.A., Wolfson, C.J., 1988, ApJ, 331, 1036

Phillips, K.J.H., Bhatia, A.K., Mason, H.E., Zarro, D.M., 1996 a, ApJ, 466, 549

Phillips, K.J.H., Greer, C.J., Bhatia, A.K., Keenan, F.P., 1996 b, ApJ, 469, L57

Mc Kenzie, D.L., 1987, ApJ, 322, 512

Mc Kenzie, D.L., Broussard, R.M., Landecker, P.B., Rugge, H.R., Young, R.M., Doschek, G.A., Feldman, U., 1980, ApJ, 238, L43

Uchida, Y., Watanabe, T., Shibata, K., Hudson, H.S. eds. 1994, X-Ray Solar Physics from Yohkoh, Universal Academy Press Inc., Tokyo

Vaiana, G.S., Davis, J.M., Giacconi, R., Krieger, A.S., Silk, J.K., Timothy, A.F., Zombeck, M., 1973, ApJ, 185, L47

Vaiana, G.S., Krieger, A.S., Timothy, A.F., 1973, Solar Phys., 32, 81

Wolfson, C.J., Doyle, J.G., Leibacher, J.W., Phillips, K.J.H., 1983, ApJ, 269, 319

Walker, A.B.C., Jr., and Rugge, H.R., 1970, A&A, 5, 4

Zarro, D.M., Slater, G.L., Freeland, S.L., 1988, ApJ, 333, L99

FIGURE CAPTIONS

Fig. 1 - R ratio (i/f) vs plasma density for O VII, Ne IX and Mg XI (From Doschek, 1990).

Fig. 2 - Line fluxes, electron density and temperature vs. time for the April 8, 1980 flare (from Doschek et al. 1981). The curves are not fittings but rather lines to guide the eye.

Fig. 3 - Electron density and temperature vs. time, during the May 21, 1985 flare, derived from the R ratio and the G ratio; the data points marked with triangles have been derived from Mg XI spectra, the crosses from Ne IX (from Linford and Wolfson, 1988).

Fig. 4 - Observed (histograms) and synthesized (smooth curves, displaced downward for clarity) spectra for different densities, for the July 2, 1985 flare. Panel a: Fe XXII spectra, over the 8.95 – 9.10 A range. (solid: 10^{12} cm^{-3}, dotted: 10^{13} cm^{-3}, dashed: 10^{14} cm^{-3}). Panel b: Fe XXI spectra over the 9.4 – 10 A range (solid: 10^{11} cm^{-3}, dashed: 10^{12} cm^{-3}, dot-dash: 10^{13} cm^{-3}) (from Phillips et al., 1996).

Fig. 5 - Evolution of plasma density vs. temperature along flaring coronal loops symmetric with respect to their apex, computed with the Palermo-Harvard code. The three vertical lines mark the temperature of maximum formation of O VII, Ne IX and Mg XI (from lower to higher temperatures); the horizontal line marks the 10^{12} cm^{-3} density. Panel a: heating centered at the loop apex; Panel b: heating located at the base of the corona. See text for more details.

Fig. 6 - Electron density and path length (in units of 10^3 km) vs. heliocentric distance (degrees) derived from the optical depth and emission measure obtained from the Fe XVII lines; (from Phillips et al. 1996b).

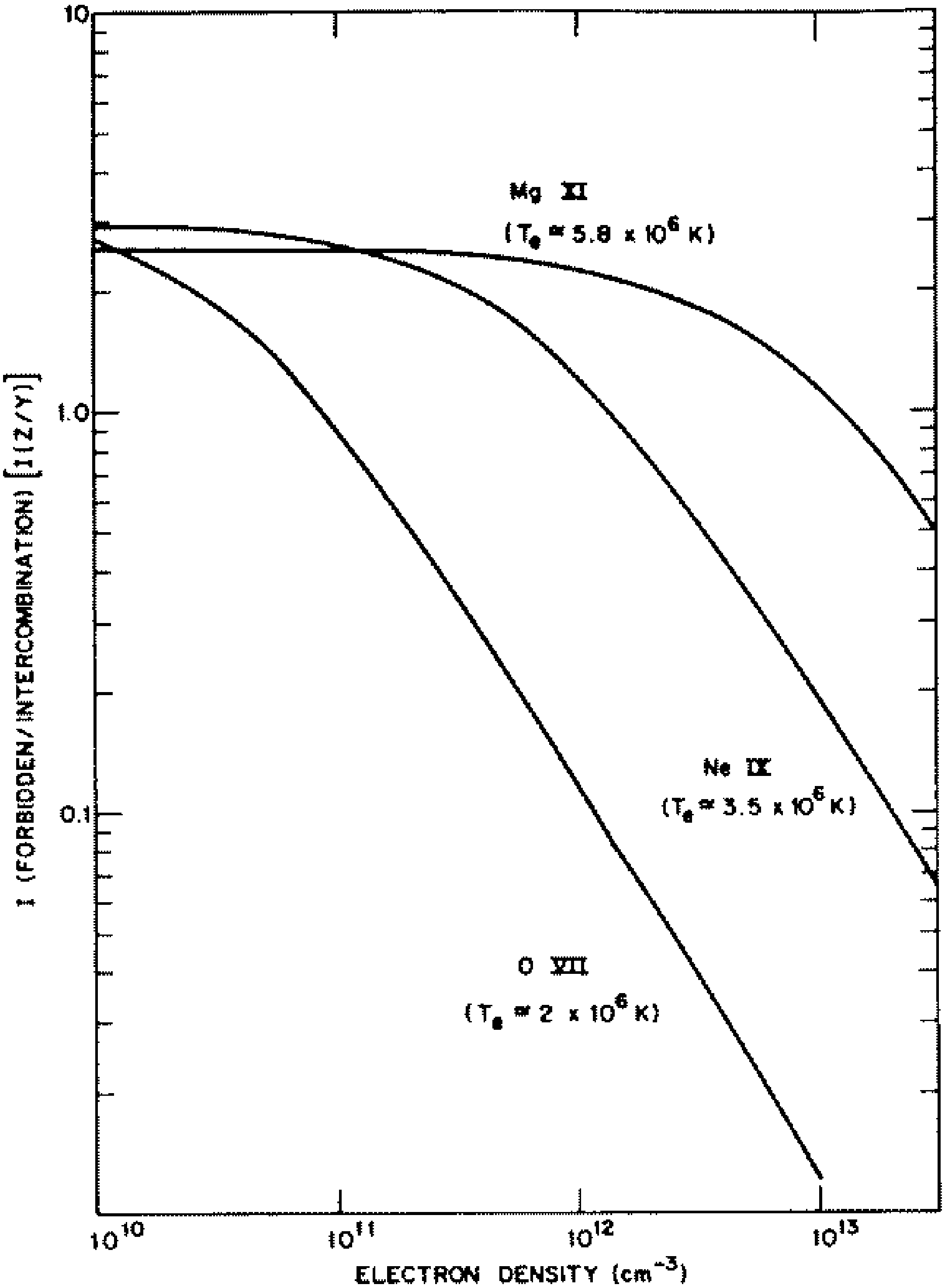

10
1.0
0.1
Mg XI
($T_e \approx 5.8 \times 10^6$ K)
Ne IX
($T_e \approx 3.5 \times 10^6$ K)
O VII
($T_e \approx 2 \times 10^6$ K)
1 (FORBIDDEN/INTERCOMBINATION) [I(Z/Y)]
10^{10}
10^{11}
10^{12}
10^{13}
ELECTRON DENSITY (cm^{-3})

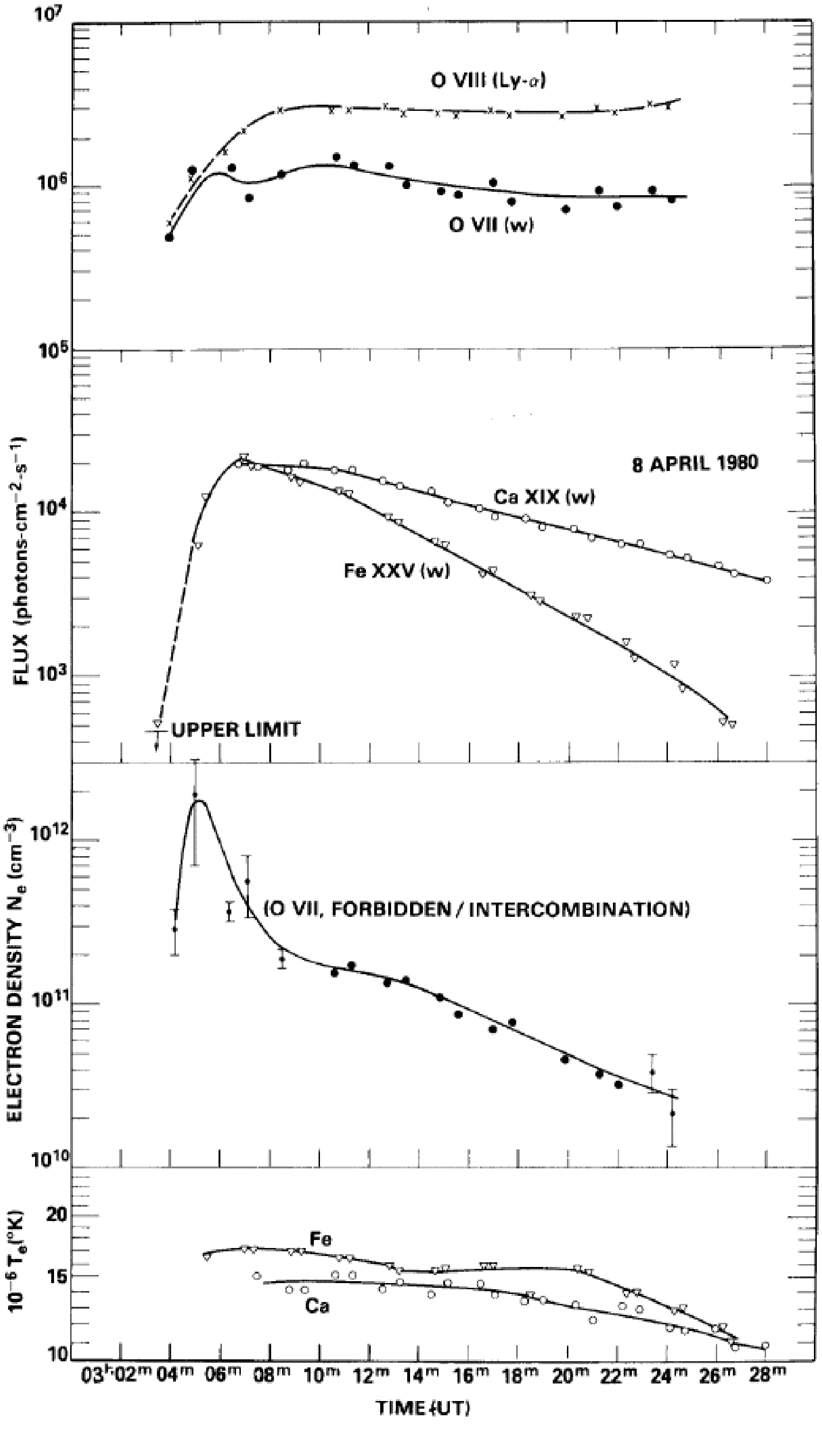

O VIII (Ly-α)
O VII (w)
8 APRIL 1980
Ca XIX (w)
Fe XXV (w)
UPPER LIMIT
(O VII, FORBIDDEN / INTERCOMBINATION)
Fe
Ca
FLUX (photons-cm⁻²-s⁻¹)
ELECTRON DENSITY Nₑ (cm⁻³)
10⁻⁶ Tₑ(°K)
TIME (UT)

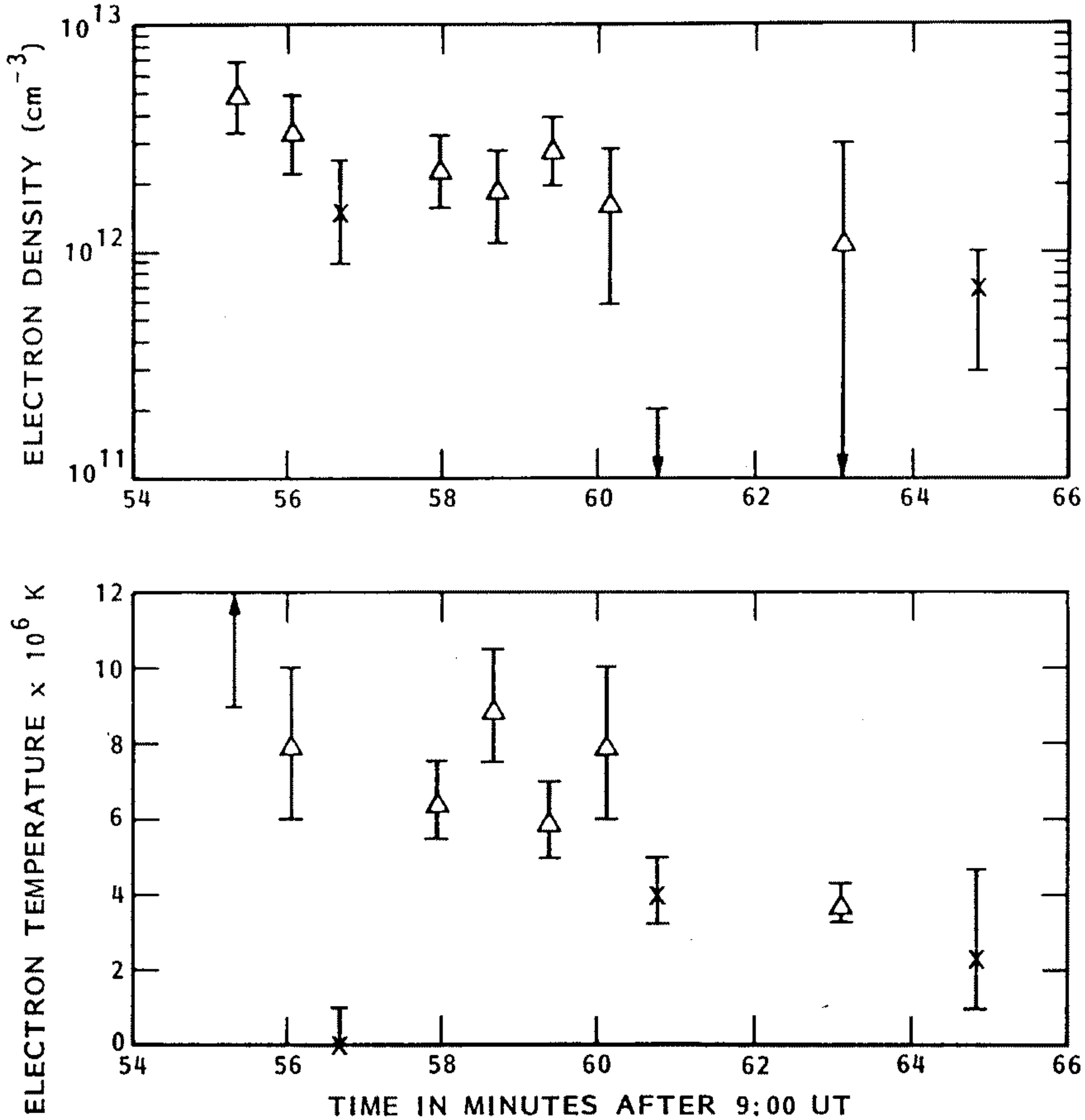

10^{13}
10^{12}
10^{11}
ELECTRON DENSITY (cm^{-3})
54
56
58
60
62
64
66
12
10
8
6
4
2
0
ELECTRON TEMPERATURE × 10^6 K
TIME IN MINUTES AFTER 9:00 UT

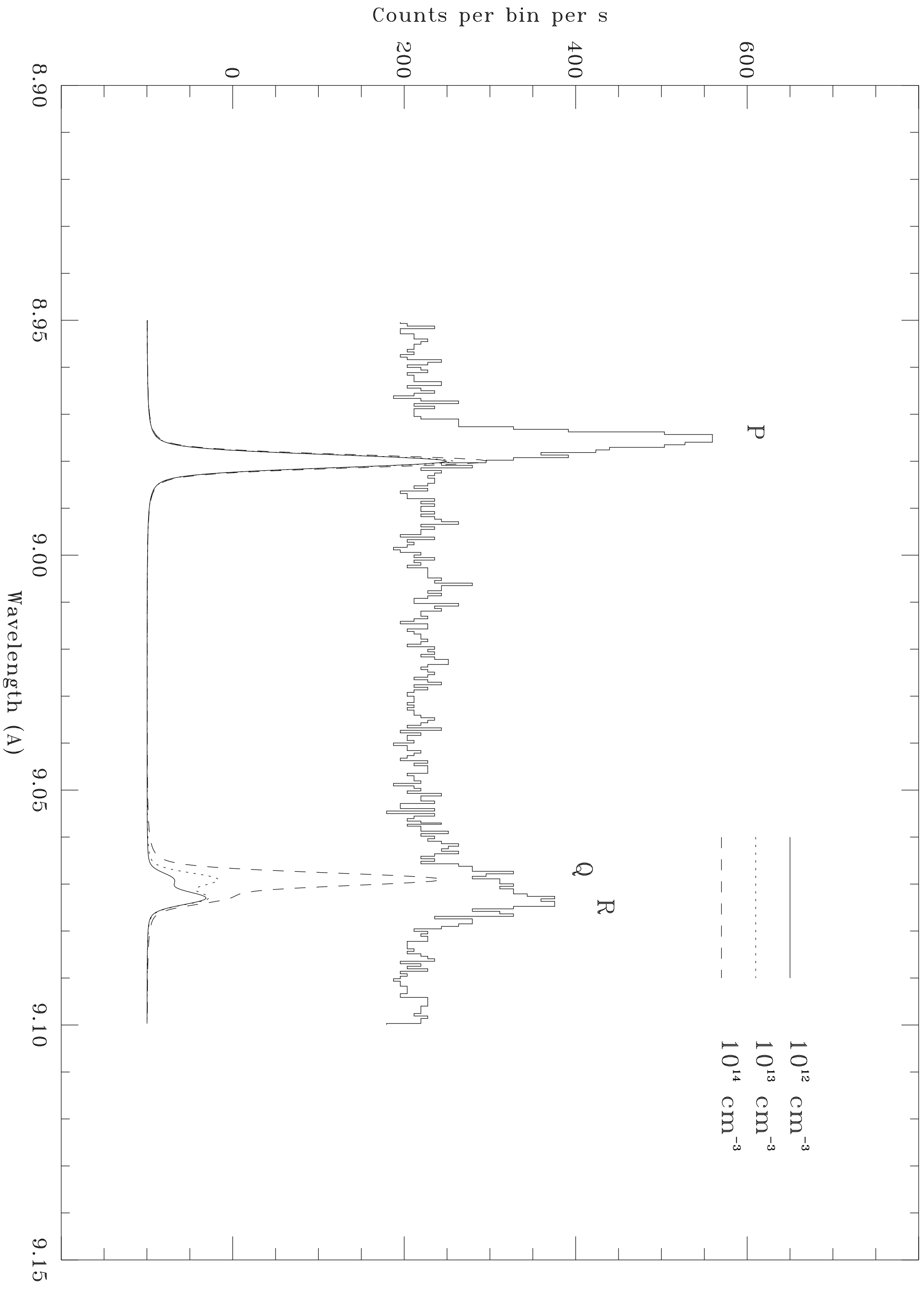

Counts per bin per s
0
200
400
600
8.90
8.95
9.00
9.05
9.10
9.15
Wavelength (A)
P
Q
R
10^{12} cm^{-3}
10^{13} cm^{-3}
10^{14} cm^{-3}

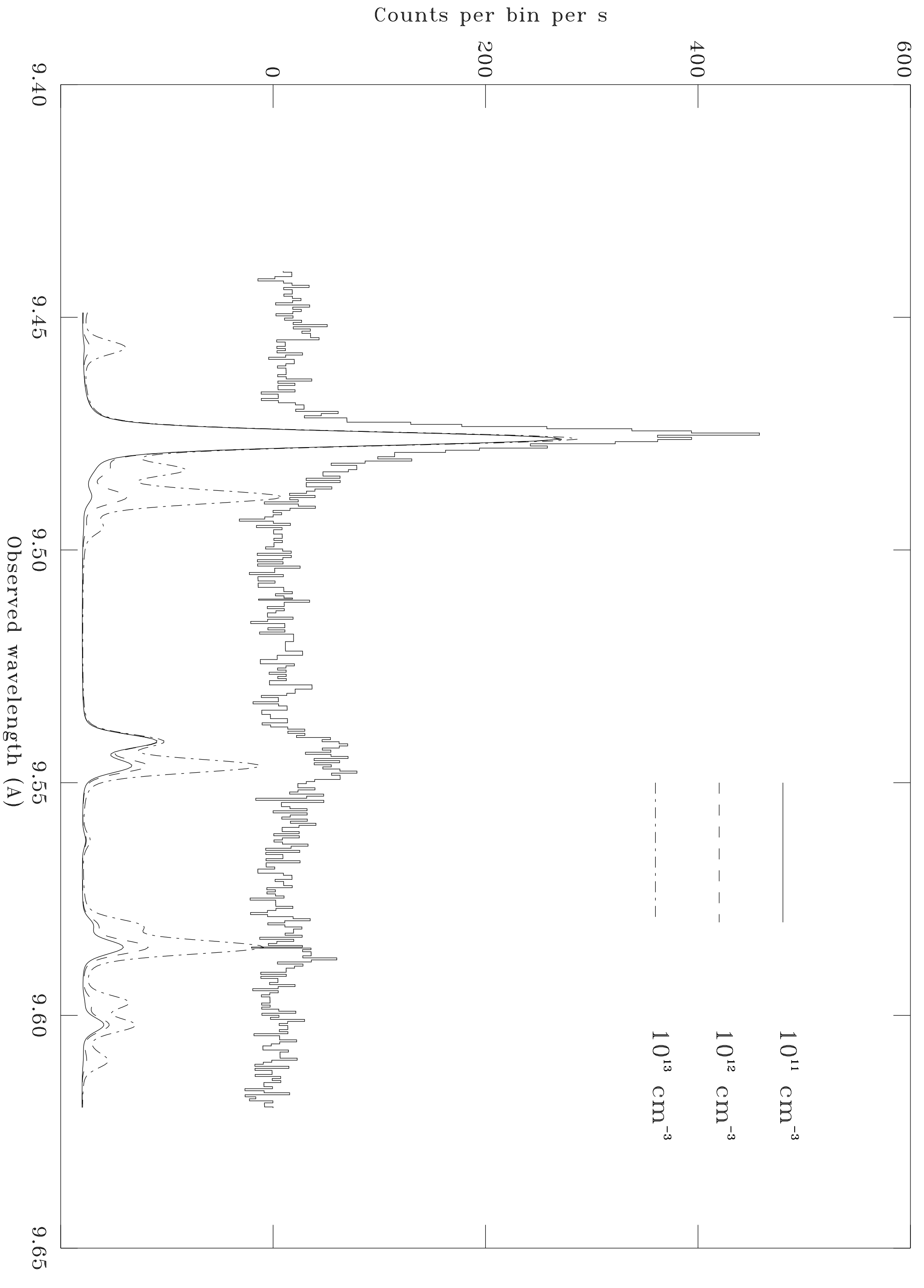

Counts per bin per s
0
200
400
600
Observed wavelength (A)
9.40
9.45
9.50
9.55
9.60
9.65
10¹¹ cm⁻³
10¹² cm⁻³
10¹³ cm⁻³

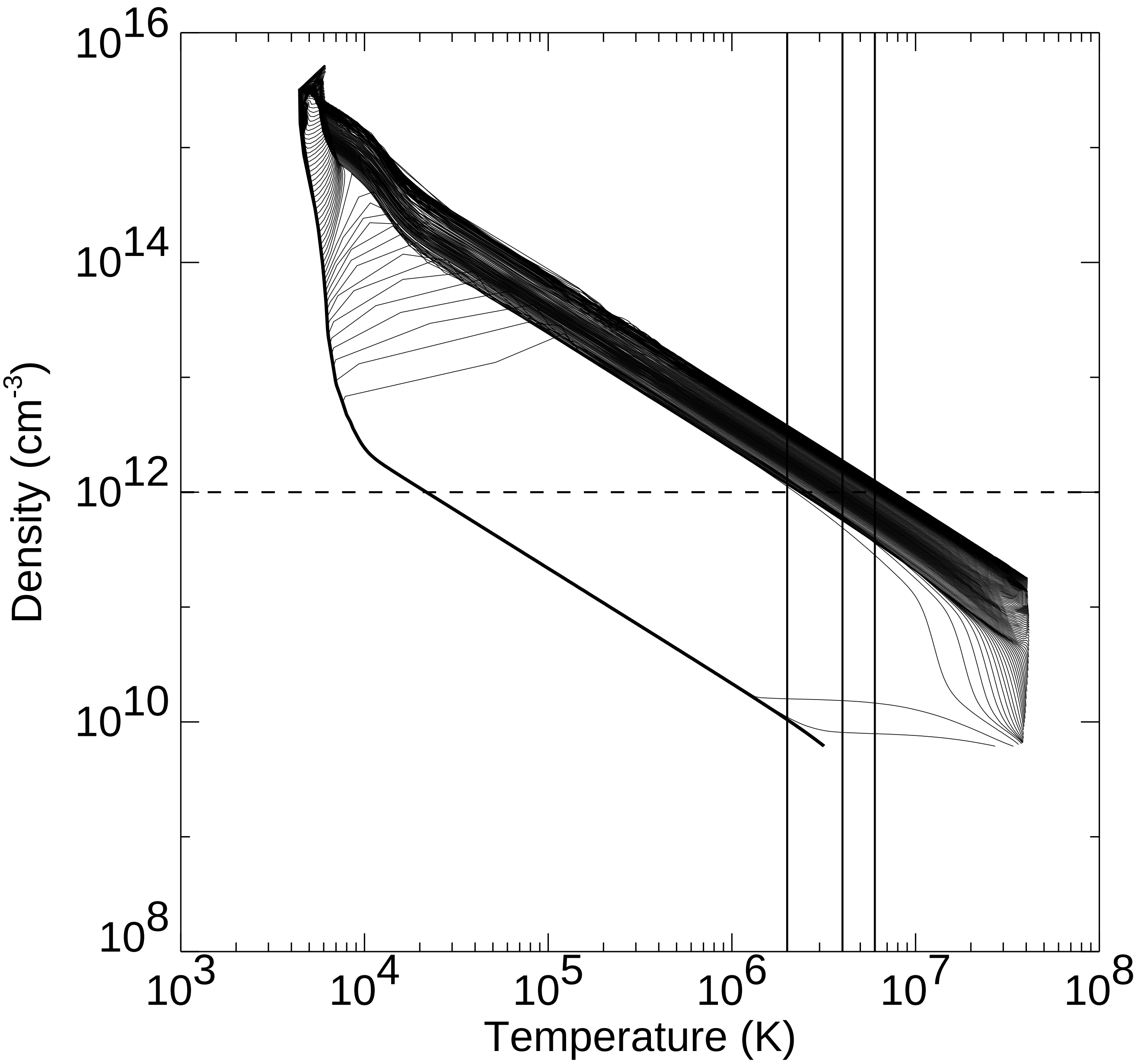

Density (cm^{-3})
10^{16}
10^{14}
10^{12}
10^{10}
10^{8}
10^{3}
10^{4}
10^{5}
10^{6}
10^{7}
10^{8}
Temperature (K)

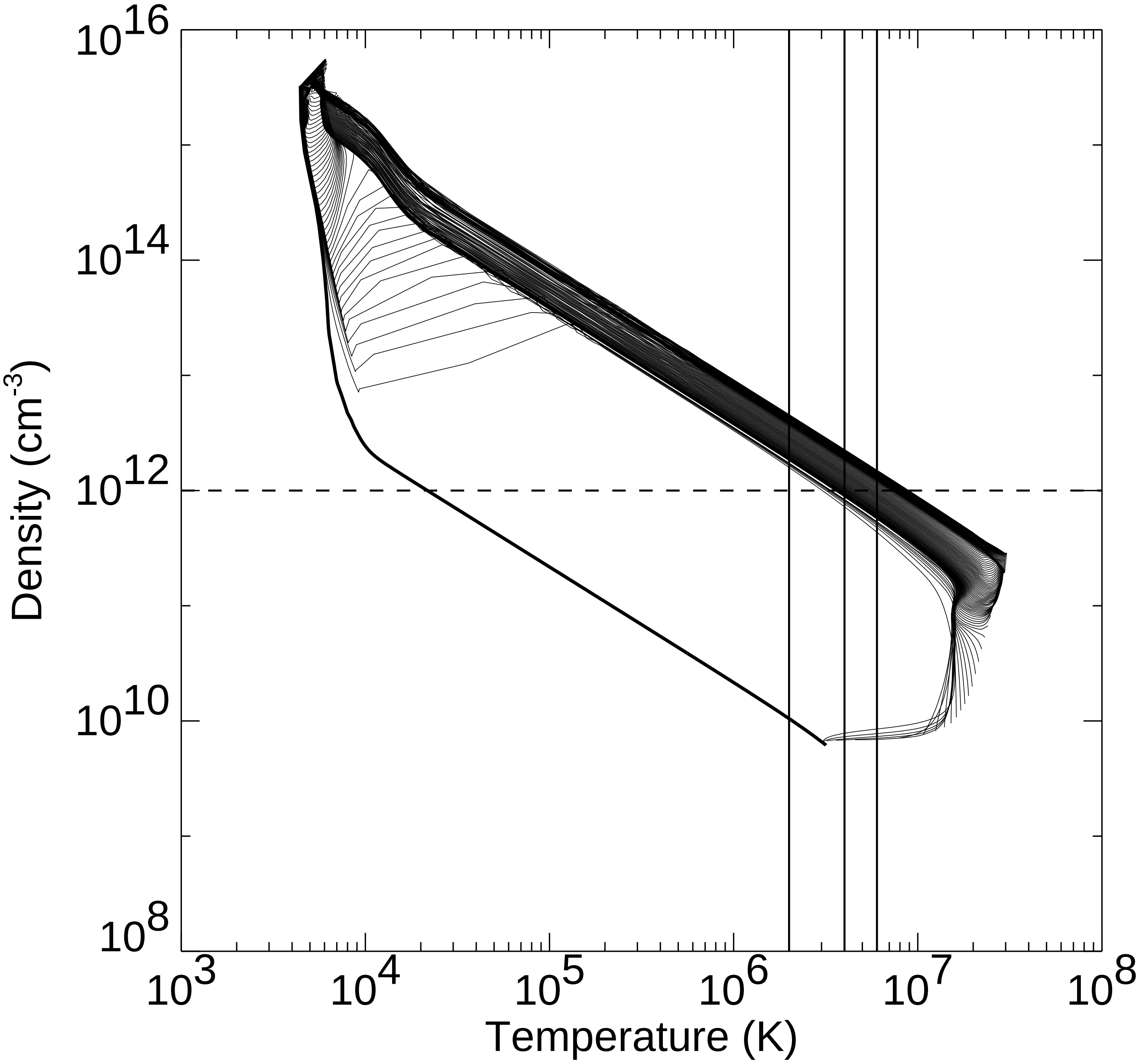

10^16
10^14
10^12
10^10
10^8
10^3
10^4
10^5
10^6
10^7
10^8
Density (cm^-3)
Temperature (K)

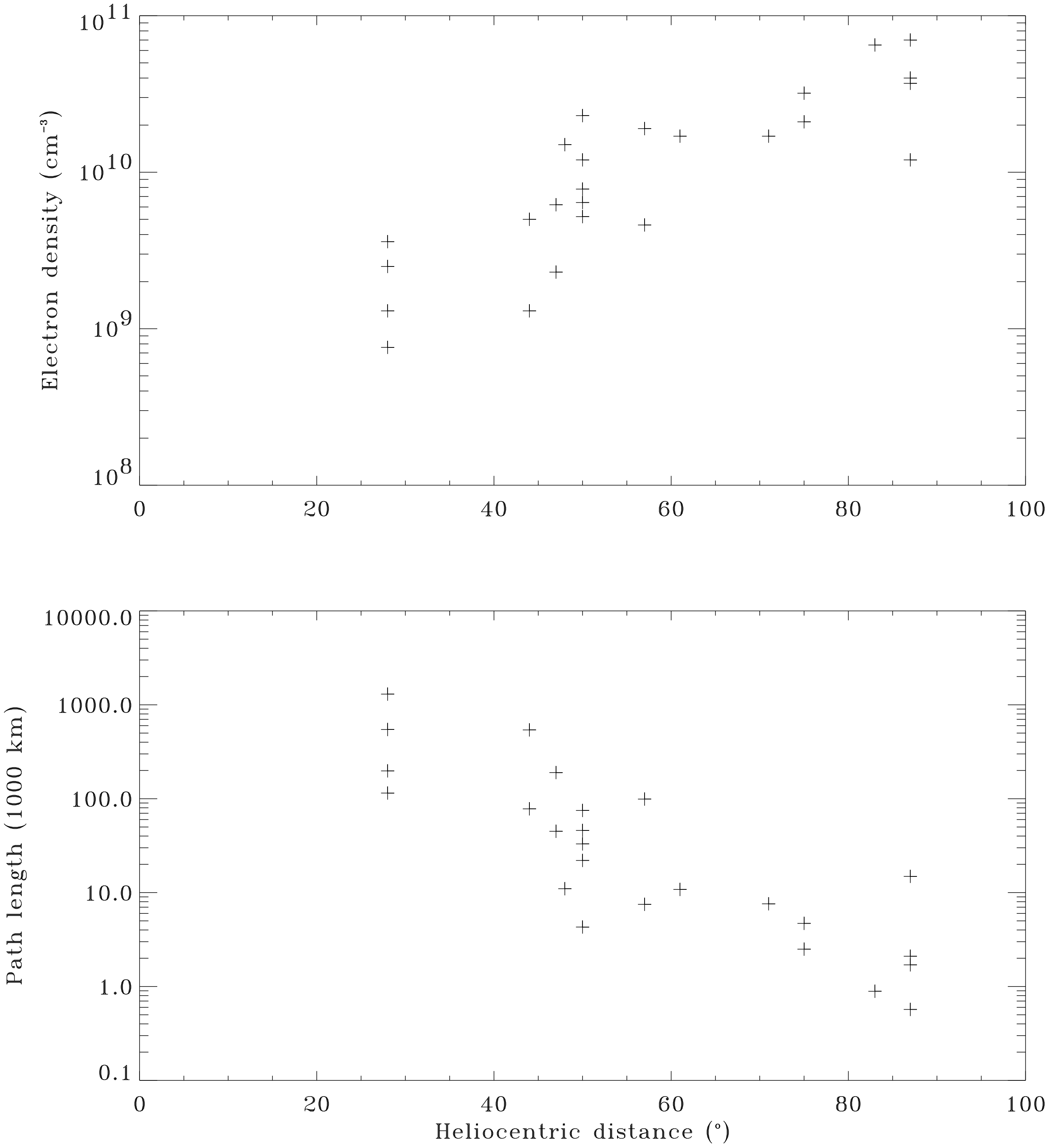

Electron density (cm⁻³)
10^11
10^10
10^9
10^8
0
20
40
60
80
100
Path length (1000 km)
10000.0
1000.0
100.0
10.0
1.0
0.1
Heliocentric distance (°)